Chemistry Letters, 2024, **53**, upad030
https://doi.org/10.1093/chemle/upad030
Advance access publication 1 December 2023

Letter

Spherulites of supramolecular polymers formed from undercooled melts, and their adhesive properties

Takuma Shimada[1,2], Yuichiro Watanabe[3], Tsutomu Furuya[3], Koji Nishida[3,*], Sadaki Samitsu[2], Yutaka Wakayama[1,2], Kazunori Sugiyasu[3,*]

[1]Department of Chemistry and Biochemistry, Graduate School of Engineering, Kyushu University, Nishi-ku, Fukuoka 819-0395, Japan

[2]National Institute for Materials Science, Tsukuba, Ibaraki 305-0047, Japan

[3]Department of Polymer Chemistry, Kyoto University, Kyotodaigaku-Katsura, Nishikyo-ku, Kyoto 615-8510, Japan

*Corresponding authors: Department of Polymer Chemistry, Kyoto University, Kyotodaigaku-Katsura, Nishikyo-ku, Kyoto 615-8510, Japan. Email: nishida.kouji.5e@kyoto-u.ac.jp, sugiyasu.kazunori.8z@kyoto-u.ac.jp

Abstract

The solid-state properties of crystalline supramolecular polymers have generally remained unexplored. Herein, we investigated the isothermal crystallization of a supramolecular polymer and showed that, depending on the temperature, it formed distinct structures at a higher hierarchical level. Interestingly, the resulting crystalline forms showed distinct adhesive properties and mechanical-failure modes (adhesive or cohesive).

Keywords: hierarchical structure, spherulites, supramolecular polymer adhesive.

Graphical Abstract

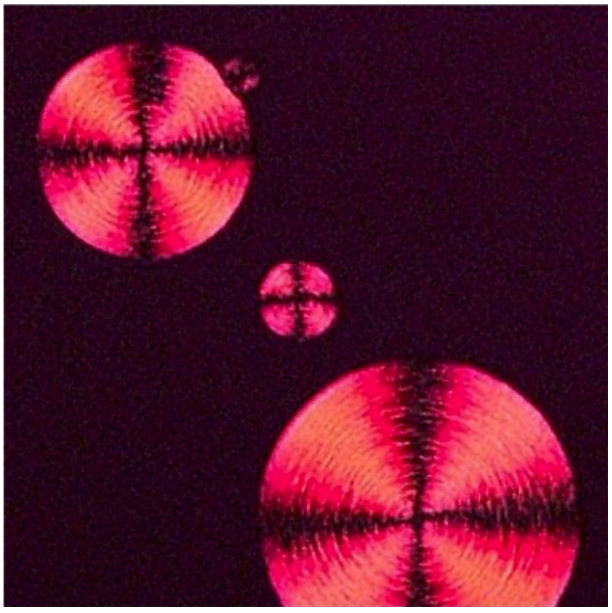

The solid-state properties of crystalline supramolecular polymers have generally remained unexplored. We investigated the isothermal crystallization of a supramolecular polymer and showed that, depending on the temperature, it formed distinct structures at a higher hierarchical level. Interestingly, the resulting crystalline forms showed distinct adhesive properties and mechanical-failure modes (adhesive or cohesive).

Spherulites are polycrystalline aggregates composed of a radiating array of crystallites[1] that frequently form from undercooled melts of crystalline polymers.[2] As such, control over spherulite formation is essential in tuning the properties of polymeric materials, such as their mechanical strength and transparency. The study described below investigates the formation of spherulites from porphyrin derivatives capable of supramolecular polymerization. Unless otherwise noted, the

[Received on 17 November 2023; revised on 26 November 2023; accepted on 27 November 2023; corrected and typeset on 19 February 2024]

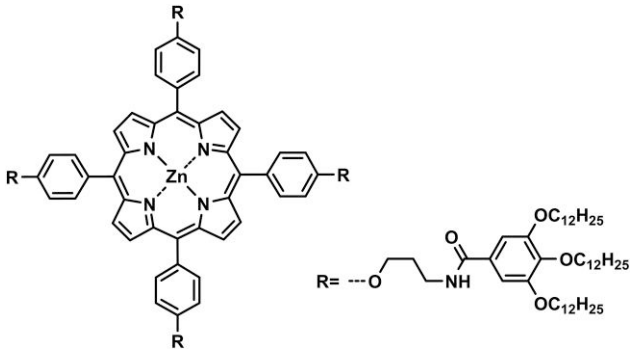

Chart 1. The chemical structure of monomer **1**.

spherulites were grown between two glass plates as radial disks with thicknesses of 11 to 12 μm.

Although spherulites of supramolecular polymers have previously been observed in solution,[3] to the best of our knowledge, there is no report of the formation of such spherulites from an undercooled melt.[4] Unlike conventional covalent polymers, supramolecular polymers "depolymerize" to their parent monomers when melted; this is expected to be advantageous for their thermal processing, due to the low viscosity of the melt. Thus far, most of the supramolecular polymers showcased as bulk materials have been amorphous: representative examples are those based on 2-ureido-4[1*H*]-pyrimidinone dimers[5] and host–guest complexes.[6] In contrast, the materials used in the present study can be categorized as crystalline supramolecular polymers. Herein, we apply the supramolecular polymer as a hot-melt adhesive:[7] we show that the mechanical strengths can be controlled by changing the processing temperature, as in the case of crystalline covalent polymers.

The porphyrin-based monomer **1** (Chart 1) was previously reported to form 1D supramolecular polymers through concerted hydrogen bonding and π-stacking in organic solvents, the process of which was characterized by a nucleation–elongation model,[8a] thus suggesting its crystalline nature. Differential scanning calorimetry (DSC) revealed that **1** forms a mesophase in a narrow temperature range (174 to 179 °C in a heating process) below that of the isotropic liquid phase (Fig. 1a): in this study, this mesophase was neither exploited nor investigated. In the cooling curve from the isotropic melt (−10 K/min), a freezing point was observed at 147 °C, accompanied by a large thermal hysteresis of ∼30 °C.

Isothermal crystallization was observed via polarized optical microscopy (POM) using a microscope equipped with a temperature-jump hot stage constructed in-house.[9] The sample cell was kept under the objective lens while the sample temperature was rapidly changed from 200 °C to a given temperature (110 to 165 °C). This resulted in undercooling of the melt, which, after a lag time, crystallized, as implied by the appearance of birefringence in the dark field under crossed Nicol (see Supplementary Information [SI]: Movie S1).

The lag time was estimated from the changes in the sum of the red value of each pixel in the POM image over time (28 frames/s [fps] and 1 fps for the blue and red curves, respectively, in Fig. 1b,c). Lower temperatures induced more rapid nucleation and, interestingly, the lag time showed a sensitive dependence on the temperature. Below 155 °C (higher degree of undercooling: Fig. 1b), crystallization was complete within 100 s and a mosaic-like texture appeared (Fig. 1d). The low contrast of the

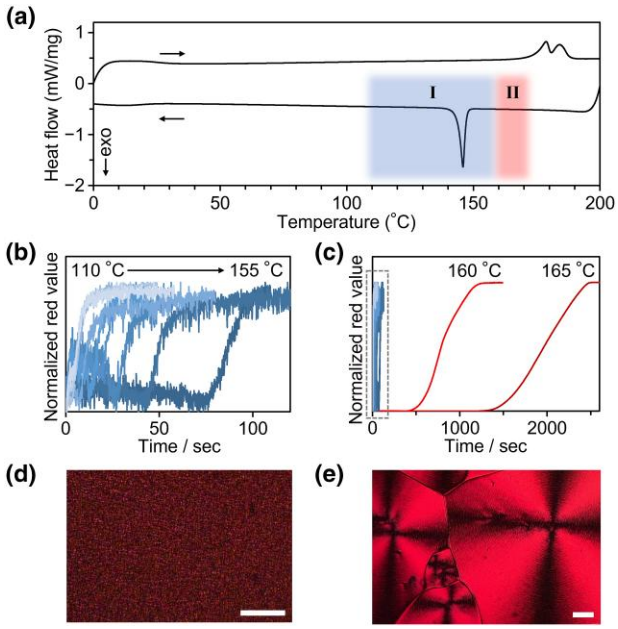

Fig. 1. a) DSC curves of monomer **1**. b), c) The kinetics of isothermal crystallization, as observed from the changes in birefringence in the time-dependent POM images. Note that the lag time for isothermal crystallization is significantly affected by the temperatures: b) below 155 °C (∼100 s) and c) above 160 °C (∼2,500 s). POM images of d) **I** and e) **II** obtained using isothermal crystallization at 130 and 165 °C, respectively, from the undercooled melt (scale bar: 100 μm).

texture indicated the absence of any long-range order. On the other hand, a much longer lag time was observed for nucleation at above 160 °C (lower degree of undercooling: Fig. 1c); in these cases, Maltese cross patterns were observed, thus suggesting the formation of spherulites (Fig. 1e and SI: Supplementary Movie S2).[1–4] The nucleation rate of the spherulites was so slow that millimeter-sized large spherulites, visible to the naked eye, were obtained (SI: Supplementary Fig. S1). From these results, we infer that supramolecular polymerization and spherulite formation are kinetically coupled in the higher-temperature range. Hereafter, the two crystalline forms described above (i.e. the mosaic and spherulite forms) are referred to as **I** and **II**, respectively.

To gain an insight into the molecular packing in **I** and **II**, their absorption and infrared (IR) spectra were recorded. In both **I** and **II**, the porphyrin molecules were found to stack in an H aggregate (i.e. face-to-face stacking) fashion with the aid of hydrogen bonding between the amide groups, as in the case of supramolecular polymers formed in organic solvents (Fig. 2a and b; SI: Supplementary Fig. S2).[8] X-ray diffraction (XRD) analysis of the two samples revealed a periodicity with a *d*-spacing of 6 nm, which is consistent with the size of **1** (SI: Supplementary Fig. S3). In addition, the DSC heat-flow curves of **I** and **II** were identical (SI: Supplementary Fig. S4). These results indicate that both **I** and **II** consist of monomer **1** in similar molecular packing. Small-angle light-scattering (SALS) measurements[10] for **II** showed a diagonal "four-leaf-clover" pattern—a characteristic of spherulites (Fig. 2d and SI: Supplementary Fig. S5b).[2,11] In contrast, **I** showed a "+ type" pattern with scattering streaks in the horizontal and vertical directions, which was attributable to the random assembly of anisotropic fibrils (rods) whose principal optical axis is tilted with respect to the long axis of the fibrils (Fig. 2c and SI: Supplementary

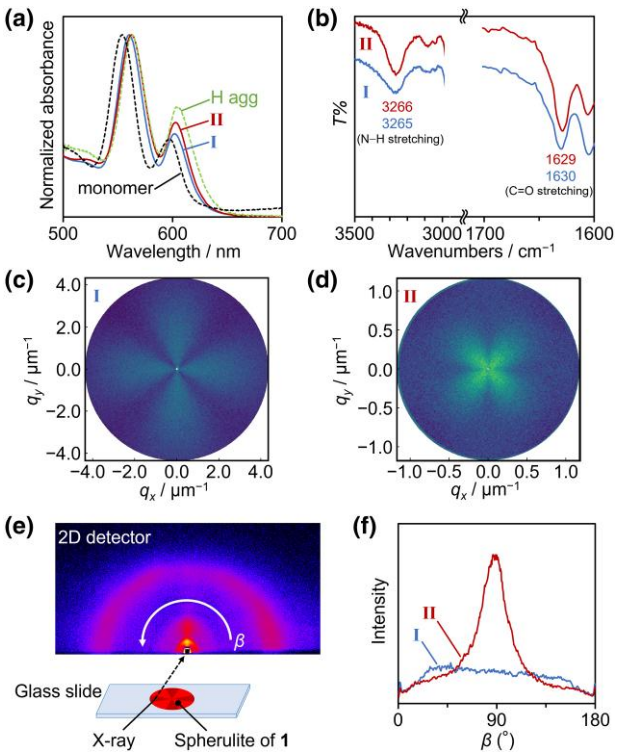

Fig. 2. a) Absorption and b) IR spectra of **I** and **II** as thin films. The dotted lines represent the monomeric state in chloroform and the H aggregate in methylcyclohexane of **1** (10 μM).[8a] SALS patterns obtained from c) **I** and d) **II** in V_H. For the SALS measurement, spherulites **II**, which were much smaller than those seen in Fig. 1d, were prepared (see SI for details). e) Schematic representation of the experimental setup for GI–XRD; (inset) the 2D diffraction pattern is that of the spherulite of **1**, obtained when the X-ray was irradiated to the edge of the spherulite. f) Angle-dependence of the peak intensity for $2\theta = 2.5°$ to 4° (approximately 3.5 to 2.2 nm; see SI: Supplementary Fig. S6) in the 2D GI–XRD with respect to β.

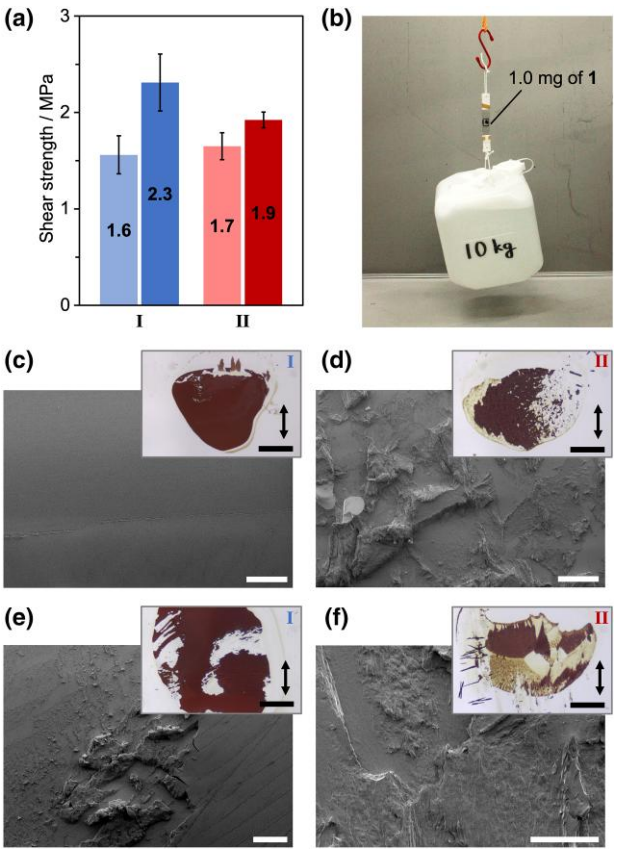

Fig. 3. a) Shear strengths of 11-μm-thick films of **1** in its **I** and **II** forms sandwiched between two glass slides (left: untreated glass slides, right: hydrophobized glass slides, respectively). b) A photograph showing the strong adhesive function of **1**. Only 1 mg of **1** in its **I** form (11 μm in thickness) sandwiched between two hydrophobic glass slides could sustain a weight of 10 kg. Photographs and SEM images of the surface of the **1** in its c), e) **I** and d), f) **II** forms on c), d) untreated or e), f) hydrophobized glass slides after the adhesion test (scale bars: 100 μm [SEM]; 2 mm [inset photograph]). The arrows show the shear direction.

Fig. S5a).[12] In addition, grazing-incidence (GI) XRD revealed that the supramolecular polymers were aligned radially in spherulites **II**, whereas they were randomly oriented in **I** (Fig. 2e,f; SI: Supplementary Fig. S6). These results suggest that the 1D supramolecular polymers of **1** formed distinct structures at higher hierarchical levels, depending on their thermal-processing conditions.

During the course of the above experiments, we noticed that the two glass plates became stuck to one another, which motivated us to evaluate **1** as a supramolecular adhesive. By controlling the temperature to 130 or 170 °C, we prepared samples of **I** and **II**, respectively, sandwiched between two untreated glass slides, and we measured their shear strength by pulling the bonded glass slides using a force gauge. **I** and **II** showed shear strengths of 1.6 ± 0.2 and 1.7 ± 0.1 MPa (Fig. 3a), respectively; these values are sufficiently high to provide temporary bonding (>1 MPa) and are comparable with those of several small-molecule-based adhesives,[13] including supramolecular polymers.[14] By using scanning electron microscopy (SEM), we examined the surfaces of the glass slides after they had been pried apart. On the surfaces of the debonded glass slides with the layer of **II**, broken spherulites were observed, suggesting that debonding had occurred within the adhesive material (Fig. 3d): i.e. partial cohesive failure.[7a,15] It appears that the large spherulites disks with well-defined interfaces showed a strong adhesion with the glass substrates (Supplementary Fig. S7), and that fracture occurs at the grain boundaries between the crystallites within the disks. Interestingly, debonding of **I**, on the other hand, occurred at the interface (Fig. 3c), i.e. by adhesive failure. The random orientation of the supramolecular polymers within the material, as suggested by the GI–XRD experiment (Fig. 2f), appears to give rise to a greater mechanical strength of the bulk material but a weaker adhesive capacity at the interface compared with **II**. These findings prompted us to examine the adhesion of **I** to hydrophobic glass slides and, gratifyingly, a shear strength of 2.3 ± 0.3 MPa was measured (Fig. 3a), corresponding to cohesive failure (Fig. 3e). This is one of the highest values obtained for a supramolecular adhesive based on a low-molecular-weight organic compound;[13,14] to our surprise, only 1 mg of **1** could sustain a weight of 10 kg (Fig. 3b). Importantly, debonding was possible by gently heating the glass slides to 140 °C. The supramolecular polymer was easily recovered from the glass slides by rinsing with an organic solvent such as dichloromethane, and the recovered material could be reused as an adhesive without any weakening of its shear strength (2.5 MPa; SI: Supplementary Fig. S8).

In conclusion, we have investigated the crystallization and spherulite formation of a supramolecular polymer from an

undercooled melt. We found that isothermal crystallization at different temperatures led to different crystalline structures. We also found that the resulting materials showed distinct adhesive properties and mechanical-failure modes (adhesive or cohesive). Further studies on the adhesion interactions at the molecular level are in progress. We believe that control over higher-order structures of crystalline supramolecular polymers could provide a basis for the development of sustainable materials.

Acknowledgments

We thank Doctors Ito (Kyoto University), Ryoki (Kyoto University), Takeuchi (NIMS), Aimi (NIMS), and Kajitani (Tokyo Institute of Technology) for fruitful discussion. T.S. thanks the Japan Society for the Promotion of Science for a research fellowship for young scientists (22KJ2440).

Supplementary data

Supplementary material is available at *Chemistry Letters* online.

Funding

This work was supported by the CREST, Japan Science and Technology Agency (JPMJCR23L2) and Grants-in-Aid for Scientific Research (JP22H02134), a Grant-in Aid for Scientific Research on Innovative Arias "Soft Crystals" (20H04682), and Data Creation and Utilization-Type Material Research and Development Project (JPMXP1122714694) from the Ministry of Education Culture Sports Science and Technology, Government of Japan. Financial support from The Iketani Science and Technology Foundation, The Murata Science Foundation, Sekisui Chemical Grant Program, and The Mitsubishi Foundation, Fujimori Science and Technology Foundation, The Samco Foundation, and Japan Society for the Promotion of Science for a research fellowship for young scientists (22KJ2440) is also acknowledged.

Conflict of interest statement. None declared.

References

1. A. G. Shtukenberg, Y. O. Punin, E. Gunn, B. Kahr, *Chem. Rev.* **2012**, *112*, 1805.
2a. B. Crist, J. M. Schultz, *Prog. Polym. Sci.* **2016**, *56*, 1.
2b. A. Keller, *J. Polym. Sci.* **1955**, *17*, 291.
3a. D. S. Pal, H. Kar, S. Ghosh, *Chem. Eur. J.* **2016**, *22*, 16872.
3b. R. Laishram, S. Sarkar, I. Seth, N. Khatun, V. K. Aswal, U. Maitra, S. J. George, *J. Am. Chem. Soc.* **2022**, *144*, 11306.
3c. M. Fontana, H. Chanzy, W. R. Caseri, P. Smith, A. P. H. J. Schenning, E. W. Meijer, F. Gröhn, *Chem. Mater.* **2002**, *14*, 1730.
3d. W. Weng, J. B. Beck, A. M. Jamieson, S. J. Rowan, *J. Am. Chem. Soc.* **2006**, *128*, 11663.
3e. W. Weng, Z. Li, A. M. Jamieson, S. J. Rowan, *Soft Matter.* **2009**, *5*, 4647.
4. In this context, the phenomena observed in this study appear to be relevant to the formation of spherulites in columnar liquid crystalline phases of discotic molecules; see M. L. Bushey, A. Hwang, P. W. Stephens, C. Nuckolls, *J. Am. Chem. Soc.* **2001**, *123*, 8157.
5. A. W. Bosman, R. P. Sijbesma, E. W. Meijer, *Mater. Today.* **2004**, *7*, 34.
6a. X. J. Loh, *Mater. Horiz.* **2014**, *1*, 185.
6b. M. Nakahata, Y. Takashima, A. Harada, *Chem. Pharm. Bull.* **2017**, *65*, 330.
7a. C. Heinzmann, C. Weder, L. M. de Espinosa, *Chem. Soc. Rev.* **2016**, *45*, 342.
7b. X. Ji, M. Ahmed, L. Long, N. M. Khashab, F. Huang, J. L. Sessler, *Chem. Soc. Rev.* **2019**, *48*, 2682.
7c. C.-Y. Shi, Q. Zhang, H. Tian, D.-H. Qu, *SmartMat.* **2020**, *1*, e1012.
8a. S. H. Jung, D. Bochicchio, G. M. Pavan, M. Takeuchi, K. Sugiyasu, *J. Am. Chem. Soc.* **2018**, *140*, 10570.
8b. S. Ogi, K. Sugiyasu, S. Manna, S. Samitsu, M. Takeuchi, *Nat. Chem.* **2014**, *6*, 188.
8c. T. Fukui, S. Kawai, S. Fujinuma, Y. Matsushita, T. Yasuda, T. Sakurai, S. Seki, M. Takeuchi, K. Sugiyasu, *Nat. Chem.* **2017**, *9*, 493.
8d. N. Sasaki, J. Kikkawa, Y. Ishii, T. Uchihashi, H. Imamura, M. Takeuchi, K. Sugiyasu, *Nat. Chem.* **2023**, *15*, 922.
8e. K. V. Rao, M. F. J. Mabesoone, D. Miyajima, A. Nihonyanagi, E. W. Meijer, T. Aida, *J. Am. Chem. Soc.* **2020**, *142*, 598.
8f. E. Weyandt, L. Leanza, R. Capelli, G. M. Pavan, G. Vantomme, E. W. Meijer, *Nat. Commun.* **2022**, *13*, 248.
9a. K. Nishida, *J. Fiber Sci. Technol.* **2019**, *75*, 145.
9b. K. Nishida, Y. Hikima, T. Koga, M. Ohshima, *Cryst. Growth Des.* **2022**, *22*, 441.
10. T. Furuya, H. Kojima, K. Nishida, Y. Fukutani, A. Mutaguchi, T. Koga, *J. Fiber Sci. Technol.* **2023**, *79*, 32.
11. R. S. Stein, M. B. Rhodes, *J. Appl. Phys.* **1960**, *31*, 1873.
12a. Y. Murakami, N. Hayashi, T. Hashimoto, H. Kawai, *Polym. J.* **1973**, *4*, 452.
12b. T. Hashimoto, Y. Murakami, N. Hayashi, H. Kawai, *Polym. J.* **1974**, *6*, 132.
13a. S. I. Stupp, V. LeBonheur, K. Walker, L. S. Li, K. E. Huggins, M. Keser, A. Amstutz, *Science.* **1997**, *276*, 384.
13b. S. Saito, S. Nobusue, E. Tsuzaka, C. Yuan, C. Mori, M. Hara, T. Seki, C. Camacho, S. Irle, S. Yamaguchi, *Nat. Commun.* **2016**, *7*, 12094.
13c. N. D. Blelloch, H. T. Mitchell, C. C. Tymm, D. W. Van Citters, K. A. Mirica, *Chem. Mater.* **2020**, *32*, 9882.
13d. S. Wu, C. Cai, F. Li, Z. Tan, S. Dong, *CCS Chem.* **2020**, *2*, 1690.
13e. X. Li, J. Lai, Y. Deng, J. Song, G. Zhao, S. Dong, *J. Am. Chem. Soc.* **2020**, *142*, 21522.
13f. S. Wu, C. Cai, F. Li, Z. Tan, S. Dong, *Angew. Chem. Int. Ed.* **2020**, *59*, 11871.
13g. J. Lai, S. Huang, S. Wu, F. Li, S. Dong, *Chem. Commun.* **2021**, *57*, 13317.
13h. M. Li, C. Xie, F. Li, X. Wang, S. Wang, Z. Qin, T. Jiao, J. Yang, *Green Chem.* **2023**, *25*, 6845.
14a. W. Zhao, J. Tropp, B. Qiao, M. Pink, J. D. Azoulay, A. H. Flood, *J. Am. Chem. Soc.* **2020**, *142*, 2579.
14b. S. Dong, J. Leng, Y. Feng, M. Liu, C. J. Stackhouse, A. Schönhals, L. Chiappisi, L. Gao, W. Chen, J. Shang, L. Jin, Z. Qi, C. A. Schalley, *Sci. Adv.* **2017**, *3*, eaao0900.
14c. J. Courtois, I. Baroudi, N. Nouvel, E. Degrandi, S. Pensec, G. Ducouret, C. Chanéac, L. Bouteiller, C. Creton, *Adv. Funct. Mater.* **2010**, *20*, 1803.
15. S. Omairey, N. Jayasree, M. Kazilas, *SN Appl. Sci.* **2021**, *3*, 769.